High-resolution modelling of ocean circulation can reveal retention spots important for biodiversity conservation

Florence Briton, Daphne Cortese, Thomas Duhaut, Katell Guizien

High resolution modelling of ocean circulation can reveal retention spots important for biodiversity conservation

Florence Briton [1] , Daphne Cortese [1] , Thomas Duhaut [2] , Katell Guizien [1, *]

[1] CNRS, Sorbonne Universités (UPMC Univ Paris 06), Laboratoire d'Ecogéochimie des Environnements Benthiques (LECOB), Observatoire Océanologique, Banyuls/Mer, F-66650, France

[2] CNRS, Université de Toulouse, Laboratoire d'Aérologie de Toulouse, 14 avenue E. Belin - Toulouse,
F-31400, FRANCE

[*] guizien@obs-banyuls.fr

ABSTRACT:

1. Larval transport by ocean circulation and its emerging property at the population level, i.e. connectivity, have received increasing attention thanks to the Aichi target 11 of protecting 10% of ocean surfaces. Furthermore, it is also important to investigate retention within a site as it determines a population's self-persistence in an isolated marine protected area.

2. Mediterranean rocky substrates host a conspicuous and diverse biota, which explains that MPA designation targetted the rocky habitat. Retention rates in the fragmented rocky habitat of the Gulf of Lion were established at two spatial scales (10- and 1-km^2) using dispersal simulations. To this end we computed three dimensionnal flow simulations with high spatial resolution nearshore (80 m) combined with a high density of release spots (every 100 m).

3. This study shows that among the six rocky 10-km^2 patches, marine protected areas (MPAs) were designated in the four ones with highest average retention rates for Pelagic Larval Duration (PLD), of up to 42 days. Furthermore, within each MPA, small zones where special protection measures are applied correspond to 1-km 2 subpatches where highest local retention rates were found. Yet, the 2% most retentive subpatches of the rocky habitat do not exhibit retention rates large enough to ensure the local persistence of most species.

Keywords: coastal, dispersal, Marine Protected Area

Introduction

Larval transport by ocean circulation and its emerging property at population levels, i.e. connectivity, have gained increasing attention in the past 10 years as displayed by the ten-fold increase in number of citations of papers refering to marine or ocean connectivity between 2005 and 2015 (Web of Science, June 1, 2017). This increase was inpart, at least stimulated by Cowen, Lwiza, Sponaugle, Paris, & Olson (2000), who questioned the broadly accepted paradigm of open marine populations. Interestingly, the beginning of ocean connectivity studies traces back to a pioneering study that linked connectivity to spatial planning of marine resources management through MPA networks (Roberts, 1997). However, to date networks of MPAs are rarely found, given that they require joint efforts of several players (local authorities, government, etc.) that are more difficult to set and manage than single MPAs promoted by local communities (IUCN-WCPA, 2008). Within such a context, it is therefore crucial to test the efficacy of single MPAs based on local retention values and in terms of ensuring species persistence through generations, in particular if new protected areas are to be designated (Halpern & Warner, 2003; Guizien, Belharet, Marsaleix, & Guarini, 2012).

Due to major advances in computing performances in the last decade, the use of ocean circulation models in ecological studies has greatly increased, providing insight at both higher spatial resolutions and broader scales compared with flow measurements. Several studies of regional connectivity for coastal species have recently been carried out using high resolution configurations of Regional Ocean Circulation Models (ROCMs) with horizontal resolutions of 1-2 km (e.g., Di Franco et al., 2012: 2.2km; Nicolle, Dumas, Foveau, Foucher, & Thiébaut, 2013: 2km; Myksvoll, Jung, Albretsen, & Sundby, 2014: 800m). Additionally, the efforts of climatologists to make high resolution downscaled versions of Global Ocean Circulation Models (e.g. NEMO-MED12 and NEMO-OPA 1/16: 6-8km) available to the scientific community has also facilitated their spread among ecologists interested in large scale connectivity studies (Andrello et al., 2013; Rossi, Ser Giacomi, Lopez Cristobal, & Hernandez-Garcia, 2014). Nevertheless, the terminology ’high resolution’ may have proved misleading in the field. ’High resolution’ refers here to the level of computing power effort devoted to the simulation – e.g., a large number of grid points to cover the simulated area - and not the actual resolution of ocean flow spatial structures. A spatial resolution of 6-8 km is currently termed ’high’ in simulations covering the Mediterranean basin while it would be termed ’coarse’ in coastal simulations. In fact, for any given level of computing effort, spatial coverage and resolution are inversely related : if one is to increase the spatial coverage, resolution would have to decrease in order to maintain the same computing effort (the reverse holds too).

Crucially, prior to performing any connectivity study using biophysical models, it is thus necessary to compromise between resolving the spatial range of the flow relevant for populations connectivity (spatial coverage) and that relevant for larval dispersal (spatial resolution).

With regard to empirical spatial coverage, although long range connections should not be totally excluded, frequent and demographically efficient larval transfer was estimated over distances ranging from 10 to 100 kms, due to the limitation imposed by larval survival (Cowen, Paris, & Srinivasan, 2006) and large-scale ocean current shaping hydrodynamical provinces (Rossi, et al., 2014). With regard to spatial resolution, larval dispersal simulations led to very different level of retention in a a bay in the south-west of the Gulf of Lion when either varying spatial resolution from 250 m to 100 m or the distance between spawning grounds and the coastline in flow simulations (Guizien, Brochier, Duchêne, Koh, & Marsaleix, 2006). Along jagged coastlines, eddies developing in the lee of capes may act as accumulative and retentive structures for particle dispersal (Denniss, Middleton, & Manasseh, 1995; Graham & Largier, 1997; Roughan et al., 2005; Mace & Morgan, 2006).

In simulations it is thus of utmost importance to resolve in 3D these flow structures in order to accurately compute larval dispersal around these geomorphological features (Doglioli, Griffa, & Magaldi, 2004). Until recently, in 3D ROCMs resolving flow equations with finite-difference numerical methods applied on cartesian grid computational limitations imposed a tradeoff between spatial resolution and spatial coverage. Nesting multiple simulations of increasing resolution and decreasing coverage was the only possibility to yield a resolution of 100 m, necessary to describe nearshore eddies (Guizien et al., 2006). The introduction of bipolar curvilinear grids transformed from Earth spherical coordinates in those ROCMs (Bentsen, Evensen, Drange, & Jenkins, 1999) enables to yield wide spatial ranges with increased spatial resolution around specified poles. Nevertheless, bipolar curvilinear grids, although allowing differential spatial resolution over the simulation domain, do not reach the meshing flexibility of models resolving flow equations with finite-element numerical method. However, up to date, those latter models have only been used in 2D depth-integrated version for regional ocean simulations (Lambrechts et al., 2008).

Besides, another important question for biophysical modellers of larval dispersal is the spatial density of particles that have to be released to account for the spatial variability of hydrodynamics. So far, particles or larvae have been released at coarse resolutions (Guizien et al., 2012: from 1/11 km^{-2} to 1/216 km^{-2} ; Di Franco et al., 2012: 1/3.25 km^{-2}; Myksvoll et al., 2014: 1/16 km^{-2}). Di Franco et al. (2012) reported that increasing the spatial density of particles did not show significant difference in dispersal trajectories given the coarse resolution (2.2 km on the horizontal) of the underlying flow simulations they used. However, a relationship between the spatial resolution of

flow simulations and the distance between release spots is to be expected, and to our knowledge its influence on retention has yet to be explicitly assessed.

The aim of the present study is to investigate the local retention and potential connectivity within the fragmented hard-bottom habitat of the Gulf of Lion (NW Mediterranean), which hosts a high biodiversity (Laubier, 1966; True, 1970; Hong, 1980) and where marine protection measures have been taken (MAPAMED, 2016). The originality of the study is to perform larval dispersal simulations using ad hoc simulations of the ocean circulation over a 100,000 km^2 area, yielding a spatial resolution of 80 m along its jagged coastline. To the best of our knowledge, these simulations feature the highest spatial resolution ever used in 3D larval dispersal studies over such large spatial coverage. This study tested the importance of resolving (1) small scale (hundreds of metres) hydrodynamical structures, and (2) spawning timing (a few days) in larval dispersal when studying retention rates. We argue that adapting the spatial and temporal resolution of ocean circulation and the seeding spatial density in larval dispersal simulations to resolve flow transport at kilometric scale provides reliable estimates of local retention and potential connectivity, with important implications for guiding marine protection extension.

Material and Methods

Area of study

The Gulf of Lion is a wide, micro-tidal continental shelf in the North-western Mediterranean, delineated by a steep shelf-break along which the Northern Current (NC, return branch of the western Mediterranean basin cyclonic circulation) flows south-westward (Millot, 1990). The infralittoral area (down to 40 m) consists mainly of soft bottoms delimited along the shore by a smooth coastline, except at its two extreme tips (Côte Bleue to the east and Côte Vermeille-Cap de Creus to the west, Fig. 1) where the coastline becomes jagged and rocky sea beds extend down to a depth of 80 m (Aloisi, Got, & Monaco, 1973). Aside these two large hard-bottom areas, only a few small areas of less than 20 km^2 are found, complementing the fragmented rocky shallow habitat (Figure 1). Coralligenous assemblages on these rocky shallow substrates host a high biodiversity (Laubier, 1966; True, 1970; Hong, 1980), including sponges, gorgonians, molluscs, bryozoans, tunicates, crustaceans and fishes. Their vast biodiversity together with their proximity to the coast makes this coralligenous habitat highly vulnerable to anthropogenic pressures such as recreational and professional fisheries (Font & Lloret, 2014), scuba-diving (Sala, Garrabou, & Zabala, 1996), and recreational boats' anchoring (Millazo, Chemello, Badalamenti, Camarda, & Riggio, 2002). In

order to protect these assemblages from anthropogenic pressure, four locally managed MPA have been designated along the Gulf of Lion coastline (Aire Marine Protégée Agathoise, Parc Naturel Marin du Golfe du Lion, Parc Marin de la Côte Bleue, and Réserve Naturelle Marine de Cerbère-Banyuls (MAPAMED, 2016).

The coastal circulation in the Gulf of Lion is a wind-buoyancy driven circulation resulting from meteorological forcings prevalence over tidal influence, with rare intrusions of the NC on the shelf under specific wind and stratification conditions (Millot & Wald, 1981; Petrenko, 2003; Barrier, Petrenko, & Ourmières, 2016). Two wind regimes can be distinguished in the Gulf of Lion: 1) strong continental northerly (Mistral) and north-westerly (Tramontane) winds that blow approximately 2/3 of time, for periods ranging from a few hours to a few days (Guénard, Dobrinski, Caccia, Campistron, & Benech, 2005), and 2) easterly and south-easterly sea winds that blow less frequently (1/3 of time) and with lower intensity (Fichaux, Poglio, & Ranchin, 2005). Despite the fact that circulation patterns related to wind regimes in the Gulf can be identified (Estournel et al., 2003), the erratic temporal variability in wind conditions translates into highly variable currents in both space and time (Petrenko, Dufau, & Estournel, 2008), with localized up- and down-wellings throughout the area (Millot, 1979; Millot & Wald, 1981; Hua & Thomasset, 1982; Johns, Marsaleix, Estournel, & Véhil, 1992), and mesoscale eddies (Hu, Petrenko, Doglioli, & Dekeyser, 2011).

Three-dimensional coastal circulation and particle tracking simulations

Three-dimensional currents were computed with the free-surface ocean model Symphonie (ver. 2015) for the extended summer period (May, 28 to November, 15) over three years (2010, 2011 and 2012). The Symphonie model solves hydrostatic primitive equations with a finite-difference method on a C curvilinear grid under Boussinesq approximation and with an energy conserving numerical scheme (Marsaleix et al., 2008). In the current configuration, turbulent closure scheme was set to two-equation K-ε (Michaud et al., 2012). Horizontal meshing was a 680 by 710 curvilinear grid with the same local resolution in orthogonal directions. The curvilinear grid was adapted to the geomorphology of the Gulf of Lion thanks to a conformal mapping (i.e., a transformation that preserves local angles) of the Earth spherical coordinates (Bentsen, Evensen, Drange, & Jenkins, 1999, details in legend of Figure 1). This bipolar grid allowed differential horizontal resolution across the domain while conserving coordinates orthogonality, with high resolution over the continental shelf in order to resolve small scale vortices and coarse resolution in the open sea in order to ensure continuity when applying matching conditions with a large-scale oceanic model at the open boundaries. Horizontal resolution ranged from 80 m along the Côte Vermeille-Cap de

Creus coastline to 400 m over the continental shelf break, to 2.7 km over the abyssal plain. The bathymetry was smoothed prior vertical meshing in order to avoid large bottom steepnesses that would create spurious vertical velocities due hydrostatic inconsistency (Beckmann & Haidvogel, 1993). Smoothing consisted in limiting relative water depth variation to 15 % between grid points applying an iterative laplacian diffusion to the initial bathymetry. Generalized σ-coordinates were used for vertical meshing, with 29 vertical levels regularly spaced for water depth lower than 100 m. For water depth larger than 100 m, the spacing between vertical levels became irregular, with a value of about 3.5 m at the surface (the vertical resolution at 100 m water depth) and increasing values towards the bottom, where spacing matched the spacing of regular σ-coordinates at that water depth. Sea surface and open-sea boundary conditions were updated every 3 h from regional downscaled climatic simulations (6-7 km horizontal resolution, NMFREE ; Hamon et al., 2016), performed at the Mediterranean basin scale by coupling the atmospherical model ALADIN forced by ERA-interim atmospherical reanalysis (12 km horizontal resolution, tri-hourly) with the oceanical model NEMO-MED12 (6-7 km horizontal resolution). Open-boundary forcings included measured discharge from the eight main rivers of the Gulf of Lion (Grand Rhône, Petit Rhône, Hérault, Orb, Aude, Agly, Têt, Tech) and the Var river in the Ligurian sea. Hydrodynamical outputs were stored at the computing grid resolution every hour for subsequent ’offline’ simulations.

Neutrally buoyant particles were dispersed ’offline’ using a pure Lagrangian approach, i.e. integrating along individual tracks, the 3D velocity field linearly interpolated in space and time between hourly discrete velocity outputs. In particular, no species-specific motility behaviour was included and dispersal duration lasted up to 42 days so as to not restrict the study to a specific species. The present study concerned larval dispersal of any species dwelling on rocky substrates and reproducing in summer, the most frequent reproductive season (D. Cortese, Personal communication). Release spots were spread evenly with a spatial density of 100/km^2 over the only rocky habitat of the Gulf of Lion (1 release spot every 100m, Figure 1). Only those locations in which flow velocity was computed according to land/sea mask were taken into account. In each spot, one particle was released 1 m above the bed (benthic species) every hour from beginning of June until the end of August, summing up to 16.2 million particles for each summer season.

Upscaling particles dispersal into connectivity matrices

Particle tracking simulations were post-processed to compute larval connectivity matrices, integrating individual tracks at the population level. A larval connectivity matrix contains larval transfer rates T_{ij} between release (rows) and destination (columns) patches. T_{ij} is the proportion of the total number of particles released in a patch i per unit area of release during a given period of

release that reach the destination patch j per unit area of the destination after a dispersal duration (the PLD). Connectivity matrices may thus vary according to : (1) the size and location of the patches they connect, and (2) the duration and timing of the release period it summarizes. Building connectivity matrices thus require choosing spatial and temporal scales of aggregation that are ecologically relevant. Hence, as initial conditions, spatial and temporal scales of aggregation were defined according to usual ecological drivers: environment fragmentation and seasonality. Larval transfer rates were computed among habitat patches delineated by expected meso-scale hydrodynamical structures and the rocky habitat fragmentation.

Six rocky habitat patches were identified in the Gulf of Lion (Figure 1, Table 1): Cap de Creus (CC, 21km^2), Côte Vermeille (CV, 4.2km^2), Cap Leucate (CL, 6.5km^2), Cap d'Agde (CA, 16.4km^2), Plateau des Aresquiers (PA, 16km^2) and Côte Bleue (CB, 10.4km^2). A larva was counted as reaching a destination patch after the dispersal duration if its position was less than 100 m of at least one of the release spots of this patch. Connectivity matrices were built for the entire summer season in three consecutive years (2010, 2011 and 2012), and for PLD ranging from 3.5 to 42 days. Local retention rates T_{ii} correspond to the diagonal of the connectivity matrix. The Relative Out-strength RO of each release patch within the patch network was defined as the proportion of out-strength (Bocaletti, Latora, & Moreno, 2010) of a patch that connects to any other patch except itself:

$$RO_i = \left(1 - \frac{T_{ii}}{\sum_{j=1}^{6} T_{ij}}\right) * 100$$

Sensitivity of retention rate to release spots spatial distribution

Given the ecological importance of local retention for population persistence (Halpern & Warner, 2003), the sensitivity of retention rates estimated at the habitat patch scale to the spatial density of release spots within the habitat patch was examined. Sensitivity analysis was performed for a 3-week PLD. To do so, the spatial density of release spots was gradually reduced by varying the distance distance (spatial resolution) from 100 m to 120 m, 200 m, 350 m, 500 m, 700 m, 1 km, 1.5 km, 2 km, 3 km and 5 km. For each spatial density (or spatial resolution) of release spots, many subsets of the original set of release spots were generated (Table 1).

For a given density of release spots to be sufficient to describe the habitat patch retention, the retention rate should not vary between the subsets of release spots. For each spatial resolution, the frequency distribution of retention rate estimates across all subsets was computed. For each habitat patch, convergence of local retention rates estimates was obtained when the frequency distribution

reaches a unimodal and narrow distribution. This is equivalent to the limit when the median value Q_{50} for the next higher resolution remains unchanged compared to current resolution, (see Supplementary Material 1 and Supplementary Figure 1). As a criteria for converging to an unimodal distribution, a threshold of 20% of uncertainty was applied, defined as the relative interquantile range $(Q_{90}-Q_{10})/Q_{50}$ with Q_{90} and Q_{10} being the 90% and 10% quantiles of the retention rate distribution, respectively.

The sensitivity of the local retention rates to the density of release spots may reflect small-scale hydrodynamical spatial structures of retention. Thus, contribution of each release spot to the retention rate of the habitat patch it belongs to was calculated and used to define subpatches in which retention rate was spatially homogeneous (see Supplementary Material 1). Finally, high spatial resolution connectivity matrices were build using 115 subpatches ranging in area from 0.16 to 1.4 km 2 (0.66 km 2 on average, Supplementary Figure 5). The cumulative area distribution of local retention rate, i.e. the proportion of the rocky surface area where local retention rate is lower than a threshold value, was computed using these 115 subpatches, for PLD ranging from 3.5 to 42 days.

Sensitivity of connectivity to release timing variability

Whilst the summer reproductive season is from June to August, species display variations in their spawning timing (e.g. among sponges: Mariani, Uris, & Turon, 2005; among gorgonians: Santangelo, Carletti, Maggi, & Bramanti, 2003, Gori, Linares, Rossi, Coma, & Gili, 2007). Furthermore, the coastal circulation in the Gulf of Lion is also driven by erratic wind regimes, leading to high spatio-temporal variability of ocean currents (Millot, 1990; Petrenko, 2003). We thus questioned if summer connectivity patterns for a week-long spawning event were predominantly driven by meteorological, seasonal or climatic (inter-annual) variability. To this end, 39 different connectivity matrices (13 per year in 3 years), each representing a non-overlapping week-long release period were built spanning the entire summer reproductive season (starting and finishing dates are given in Supplementary Table 1). The variability of larval transfer probabilities at various temporal scales (within month hereinafter called $Var_{intra\text{-}month}$, within season hereinafter called $Var_{intra\text{-}summer}$,and between years hereinafter called $Var_{inter\text{-}summer}$) was computed as defined in see also Supplementary Material 2.

Results

Average summer connectivity among rocky habitat patches

The average summer particle flows among the six main rocky habitat patches of the Gulf of Lion were less than a few percent, and heterogeneous, regardless of the duration of dispersal (Figure 2). The average connectivity pattern revealed two types of habitats: « closed» ones with retention rate larger than export rates (relative out-strength lower than 50 %), and « open » ones with export rates larger than retention rate (relative out-strength larger than 50 %). After seven days of dispersal, retention rate clearly dominated over export rate in Cap de Creus, Côte Vermeille, Cap d'Agde, Plateau des Aresquiers and Côte Bleue with retention rate values of 3.39, 1.65, 1.40, 0.89 and 1.94%, respectively (Figure 2A), and relative out-strength values RO ranging from 0 to 34% (Table 1). Conversely, Cap Leucate exhibited a much lower retention rate value of 0.15 % and a high relative out-strength value (RO = 74 %), transferring particles predominantly to Côte Vermeille (0.22 % after 7 days of dispersal). The connectivity matrix for a 7-day Pelagic Larval Duration (PLD) was fairly symetrical. It displayed three clusters of rocky habitat patches formed by closest neighbouring patches exchanging a proportion of particles comparable to the proportion that remained in their release grounds (more than 0.2 %): one cluster included Cap de Creus, Côte Vermeille and Cap Leucate, another cluster included Cap d'Agde and Plateau des Aresquiers, while Côte Bleue was disconnected from these two former clusters (Figure 2A).

Increasing the PLD up to 21 days, retention rate values decreased in all habitat patches, yielding 1.43, 0.60, 0.05, 0.50, 0.08 and 0.74 % from west to east (Figure 2B and 3). However, only Plateau des Aresquiers rocky habitat shifted from a closed to an open habitat patch, with relative out-strength increase from 33% to 82% (Table 1). In Cap de Creus, Côte Vermeille, Cap d'Agde and Côte Bleue, retention remained dominant over export for a 21-day PLD (Figure 2B). Nevertheless, relative out-strength increased in eastern habitat patches thanks to an increase in long distance connections within the Gulf of Lion while it decreased in the western habitat patches due to a decrease of the transfer rate to closest neighbours and export out of the Gulf of Lion (Table 1). The connectivity matrix became asymmetrical, with a dominant North-east to South-west particle flow (higher transfer rates above the diagonal, Figure 2B) and the three clusters of preferentially connected habitat patches for a 7-day PLD merged into a single cluster when PLD was set to 21 days. Yet, it is noteworthy that Côte Bleue received a very low proportion of particles from the other habitat patches of the Gulf for a dispersal duration up to 42 days (data not shown, incoming transfer rates ranged between 10^{-4} and 10^{-3} % for a 21-day PLD). In contrast, outgoing transfer rates from Côte Bleue to all other habitat patches were one order of magnitude higher than incoming transfer rates. For PLD lower than 14 days, Côte Bleue was only supplying the closest neighbouring habitat patch, namely Plateau des Aresquiers. For dispersal duration larger than 14 days, this pattern

was reversed: the closer the habitat patch is to Côte Bleue, the fewer particles it received, with Côte Bleue now mainly supplying the Cap Creus, the furthest from Côte Bleue (transfer rates from Côte Bleue to Cap de Creus, Côte Vermeille, Cap Leucate, Agde and Plateau des Aresquiers respectively being 0.026; 0.017; 0.017; 0.008; 0.004 % after 42 days of dispersal).

Retention rates (the diagonal of a connectivity matrix) decreased rapidly up to a 21-day PLD and reached a stable value for longer dispersal duration in all habitat patches, except in Cap Leucate in which retention rate was always small (Figure 3). The habitat patch ranking with regard to retention rate was maintained for all dispersal durations, Cap Creus being the most retentive, followed by Côte Vermeille, Côte Bleue, and Cap d'Agde, than Plateau des Aresquiers and last, Cap Leucate. Yet, average retention rate values should be taken with caution as retention rates varied significantly among the different release periods of three consecutive summers (2010, 2010 and 2012) with standard deviation yielding 100% of the mean in all habitat patches and for all dispersal durations.

Meteorological variability during release period drives connectivity

Seasonal variability (between different months of reproduction within a year, $Var_{intra-summer}$) and climatic variability (between the same month of reproduction in different years, $Var_{inter-summer}$) had the same order of magnitude, whatever the dispersal duration (Figure 4A). Their ratio for any of the 36 pairwise transfer probabilities among the six habitat patches ranged from 0.3 to 2.6, whatever the dispersal duration. Neither seasonal nor climatic variability dominated for dispersal durations of up to 21 days (median of the 36 values of the ratio between climatic and seasonal variability was close to 1). When dispersal duration increased from 21 to 42 days, climatic variability started to exceed seasonal variability (median of the 36 values of the ratio between climatic and seasonal variability larger than 1). This was the case in 26 out of the 36 possible pairwise connections among the six habitat patches for a dispersal duration of 35 days.

In contrast, meteorological variability (between release periods within each month of reproduction, $Var_{intra-month}$) clearly outweighted seasonal variability in all pairwise connections among the six habitat patches for dispersal durations of up to 21 days (Figure 4B), with an effect as large as 7.8 times larger than the seasonal variability. The dominance of meteorological variability over seasonal variability was observed for all dispersal durations, although decreasing when dispersal duration increased: the median of the 36 values of the ratio of meteorological to seasonal variability varied from 3 to 4 for PLD lower than 21 days and dropped below 2 for PLD larger than 21 days.

Coastline indentation drives retention rates patchiness down to 1km^2 scale

Retention rate estimates varied according to the density of release spot, but did so differently according to habitat patches. While retention rate estimates did not vary much with release spot distance in the Plateau des Aresquiers and Cap Leucate, uncertainty on retention rate estimates notably decreased

when distance between release spots decreased below 1 km in Cap de Creus, Cap d'Agde, Côte Bleue and Côte Vermeille, with a faster reduction of uncertainty in Cap de Creus than in the three other habitat patches (Figure 5B). The distance between release spots required to reach a precision of 20 % in retention rate estimates among different release spot subsets (relative interquantile range less than 20%) was 700 m in Plateau des Aresquiers, 350 m in Cap Leucate and 200 m in Cap de Creus, while it was 100 m in Cap d'Agde and Côte Bleue. In Côte Vermeille, with a distance of 100 m between release spots, the precision of 20 % around the median could not be obtained and the deviation between the 10 % and 90 % quantiles was 35%.

Stabilization of the median retention rate values was reached for a distance between release spots of 250 m in all habitat patches except in Côte Vermeille (deviation by less than 5% between median retention rate values for release spot spatial resolution of 100 m and 250 m, Figure 5A). In Côte Vermeille, median retention rate still exhibited 25% deviation between the 120 m and the 100 m release spots spatial resolution. However, such a deviation was four times lower than the variability among retention rate values at different release periods (Figure 3).

The large uncertainty on retention rate estimates when distance between release spot was larger than 1km in Cap Creus, Côte Vermeille, Cap d'Agde and Côte Bleue (Figure 5A) indicated that retention rates could vary greatly over a 1 km distance within these habitat patches (Supplementary Figures 2, 3 and 4 and Figure 6). Retention rates computed within 115 subpatches of about 1 km^2 (defined in Supplementary Figure 5) showed highly retentive subpatches in Cap Creus, Côte Vermeille, Cap d'Agde and Côte Bleue with retention rates greater than 2% for a 21-day PLD. Crucially, those subpatches correspond to locations where special marine protection is implemented (Figure 6). The highest local retention rate was found in one subpatch of Cap de Creus, ranging from 5% for a 7-day PLD to 3.5% for a 42-day PLD. Altogether, in the Gulf of Lion, local retention rate was higher than 5% in only 6.8% of the rocky surface area for PLD of 3.5 days (data not shown), and equal or lower to 5% everywhere in the rocky habitat for PLD equal or larger to 7 days (Figure 7). For a PLD of 7 days, local retention rates was less than 2 % over 90 % of the rocky surface area and less than 4 % over 98 % of the rocky surface area (Figure 7). For PLD larger than 7 days, local retention rates was less than 1.5 % over 90 % of the rocky surface area and less than 2.5 % over 98 % of the rocky surface area .

Average connectivity matrices at high spatial resolution (that is, among the 115 subpatches, Figure 8) further indicated that highly retentive subpatches (displayed by vertical stripes in Figure 8C and D) corresponded as well to sink areas that received particles from neighbouring or distant subpatches (displayed by vertical stripes in Figure 8A and B). Conversely, source subpatches displayed by horizontal stripes could be both retentive and non-retentive. It is worth noting that regardless of the PLD, transfers within subpatches of the southern part of Cap de Creus were high and bidirectional. On the other hand, the direction of transfer to distant habitat patches varied with the PLD. For a 7-day PLD, the southern part of Cap de Creus spread a higher proportion of particles to the Côte Vermeille than it received from it. For a 21-day PLD, it received particles from up to Cap d'Adge but spread only to Cap Leucate.

Discussion

The present study shows the strong spatial heterogeneity in local retention rates estimated at a scale of 1 km^2 around a jagged coastline. The results reported here highlight the inadequacy of low resolution flow simulations produced with global ocean climatic models for tackling the question of retention in coastal MPAs (Andrello et al., 2013). Criticisms as to the realism of the in silico approach of larval dispersal has mainly focused on the assumptions restricting larvae to neutrally-buoyant particles, disregarding their motility behaviour (Cowen et al., 2006), ontogenic development (Guizien et al., 2006) or mortality (Cowen et al., 2000). Furthermore, incorporating this information is still currently limited by gaps in biological knowledge. Notwithstanding the importance of such biological aspects in altering dispersal patterns, the choice of spatial and temporal resolutions of ocean flow simulations in larval transport studies should be questioned (Putman & He, 2013). For instance, spatial resolution as low as tens of metres were used to depict flow variability in reef mosaic or complex costalines (Andutta, Kingsford, & Wolanski, 2012; Herbert et al., 2012). Yielding such spatial resolution in flow simulations covering an area of hundred of square kilometers representative for populations connectivity was only achievable in 2D finite-element models. Yet, coastal flows influenced by wind forcing are not accurately resolved with 2D models, and 3D models able to resolve Ekman layers should be used (Petrenko et al., 2008).

Until recently, 3D models based on a finite-difference numerical scheme were limited by their regular orthogonal meshing and required successive nested meshes to improve spatial resolution (Blayo & Debreu, 1999). However, nested meshes can complicate particle tracking when they

disperse outside the smallest nested domain and return to it thanks to meso-scale eddies (Guizien et al., 2006). In the present study, such retention processes were observed in rocky patches located a few kilometers offshore (Cap Leucate and Plateau des Aresquiers) and resulted in evenly distributed retention rates. The latter *a posteriori* justifies the coarse 750 m horizontal resolution used in Guizien et al. (2012) to study soft-bottom species dispersal. Conversely, on other rocky patches retained particles did not leave the habitat during their entire dispersal, regardless of the PLD used. In those patches, retention resulted from either simulated weak flow velocities due to important bottom friction in shallow areas in Cap d'Agde or from simulated retention structures with spatial scales less than 200m in the lee of capes or in bays along the steep bathymetry of Côte Bleue, Côte Vermeille and Cap de Creus.

Such small scale structures could not be simulated in a previous study using the same model but with a 750 m horizontal resolution. Very low retention rates were reported in large soft-bottom areas (11 to 216 km^2), spanning water depths of 10 to 30 m, at three of the four rocky habitat patches investigated (Guizien et al., 2012). Increasing horizontal resolution by a factor of about 10 in the same numerical model enabled simulation of small scale hydrodynamical structures important for retention in rocky habitat patches adjacent to jagged coastlines and nearby soft bottoms. Hence, incorporating curvilinear meshing into 3D finite-difference models such as the one used in the present study opens the way for improved horizontal resolution in 3D ocean flow simulations used for larval dispersal studies. This is of particular interest where the geomorphology imposes high horizontal resolutions, in order to avoid computationally costly nesting procedures.

Nonetheless, one has to keep in mind that the true resolution of flow structures in ocean models may be different from the theoretical grid resolution. Numerical schemes used to discretize primitive equations constrain the effective resolution of flow dissipation and may alter flow representation in simulations (Soufflet et al., 2016). However, in the absence of ground truth validation versus flow measurements, larval dispersal simulation reliability is difficult to estimate. For instance, high retention rates in isolated locations very close to the coast are most likely artifacts: in the absence of a hydrodynamic calculation point between a release spot and the coast, the logarithmic decay of flow velocity in the coastal boundary layer will be linearly interpolated and the flow underestimated. Conversely, can several release spots spaced a 100 m from each other (more than grid resolution) along the Côte Vermeille consistently depicting high retention rate be considered as a reliable indicator of the existence of actual retention ? Strikingly, the four rocky habitat patches with highest average retention for PLD up to 42 days, namely Cap de Creus, Côte Vermeille, Cap d'Agde and Côte Bleue correspond to areas designated for marine protection in the

Gulf of Lion. Furthermore, areas with highest average local retention at the 1-km^2 scale in Cap d'Agde and Côte Bleue, and partially in Côte Vermeille, correspond to areas where special marine protection have been implemented. Given that the present study quantified for the first time the retention in those places, this criterion was not used in their designation. Until now, MPA designation has been largely based on the biotic richness of areas. Persistence of high biomass and biodiversity in some locations indicates that in those locations, many species reached local equilibrium, that is, colonization compensated local extinction. For species with a dispersive larval stage which can potentially form metapopulations (Levins, 1969), colonization can result from either local retention or import from distant populations. Both local retention rates as well as import rates were higher in the small subpatches where marine protection had been designated based on biotic richness. These finding validate the present simulations.

Designating areas with high local retention for marine protection is essential for at least two reasons. On the one hand, such areas are highly vulnerable to contaminations. In a context of limited dispersal, low dilution of organic or inorganic effluent is likely to lead to local eutrophication and/or anoxia (Xu et al., 2010). On the other hand, such areas are the ones where self-persistence of isolated populations can be expected. Hence, we advocate using biophysical models with adequate spatial resolution to identify areas with high local retention to help guide future marine spatial planning. Meanwhile, verifying that highly retentive areas effectively ensure population self-persistence requires comparison of retention rates with the threshold defined by species life-history traits. Neglecting losses during recruitment (taking a recruitment success equal to 1, Hastings & Botsford, 2006), local retention rates should be ranging from 5.9 to 14.4% to ensure population self-persistence for species with 3-yr life expectancy, a fecundity of 10^4 eggs per adult and a PLD ranging from 1 to 4 weeks (Guizien et al., 2012). Hence, self-persistence of species with such life-history traits would not be achieved in any subpatch of the rocky habitat of the Gulf of Lion. However, for a PLD ranging from 5 to 6 weeks and a fecundity of 10^5 eggs per adult, population self-persistence would be yielded in about 2% of the rocky surface area, although still ignoring losses during recruitment. Indeed, increasing the coverage of no-take zones in the Mediterranean Sea from the current value of 0.04% to 2% by 2020, targeting key functional areas is the objective set up during the 2016 MEDPAN Forum (Tangier declaration, http://www.medmpaforum.org/sites/default/files/tangier declaration.pdf). Meanwhile, keeping in mind that recruitment success is by definition less than 1, this means that even if marine protection designation was directed towards those most retentive areas, self-persistence may not be achievable for species whose life-history traits impose much higher local retention rates than the flow allows. In such cases, populations persistence at a regional scale would rely on connectivity among distant

subpatches forming persistence loops over multiple generation (Hastings & Botsford, 2006). Indeed, achieving species conservation objectives in the fragmented rocky habitat of the Gulf of Lion relies on the identification of networks of connected subpatches. Indeed, protecting source populations providing larvae to unprotected populations (identified by horizontal stripes in connectivity matrices), may prove completely unefficient if those source populations do not maintain themselves through receiving sufficient larvae. Yet, protecting sink populations receiving larvae from unprotected populations is even more cynical. In addition to being unefficient because depending on the wealth of unprotected supplying populations, it may give a false impression of protection efficiency as sink populations have a higher resistance to local perturbations. Designating efficient MPAs requires to go beyond the easy identification of source and sink populations from connectivity patterns, by investigating the populations network functionning within a region. To this aim, the present study provides ready-to-use connectivity matrices among 1-km^2 rocky subpatches to analyze the persistence of rocky populations in the Gulf of Lion through metapopulation modeling, accounting for demographical processes (Moilanen, 2011) . Such an approach will enable to evidence the minimal set of populations necessary to achieve conservation objectives and test future maritime spatial planning scenarios including MPA extension (Guizien, Belharet, Guarini, & Moritz, 2014 ; Padron & Guizien, 2016).

Acknowledgements

This work was funded by the French National Program LITEAU IV of the Ministère de l'Ecologie et de l'Environnement Durable under project RocConnect - Connectivité des habitats rocheux fragmentés du Golfe du Lion (PI, K. Guizien, Project Number 12-MUTS-LITEAU-1-CDS-013). The authors particularly thank the scientific managers of the Gulf of Lion MPAs : S. Blouet, E. Charbonnel, B. Ferrari and J. Payrot for valuable interactions in the study design. The Symphonie ocean model is developed by the SIROCCO group. Sources are available at http://sirocco.omp.obs-mip.fr/outils/Symphonie/Sources/SymphonieSource.html. We thank S. Somot (METEO FRANCE) for supplying the atmospheric forcings, J. Beuvier (MERCATOR-OCEAN) for supplying the NEMO-MED12 large-scale circulation forcings, and the Banque Hydro (http://www.hydro.eaufrance.fr/) for supplying rivers discharge data. We also warmly thank L. Bramanti for critical comments on the manuscript.

LITERATURE CITED

Aloisi, J.C, Got, H., & Monaco, A. 1973. Carte géologique du précontinent languedocien au 1/250000ième. Netherlands : Enschede : International Institute for Aerial survey and Earth sciences. (ITC), Netherlands.

Andrello, M., Mouillot, D., Beuvier, J., Albouy, C., Thuillier, W., & Manel, S. 2013. Low Connectivity between Mediterranean Marine Protected Areas: A Biophysical Modeling Approach for the Dusky Grouper. *Plos One*, 8(7), e68564.

Andutta, F.P., Kingsford M.J., & Wolanski, E. 2012. 'Sticky water' enables the retention of larvae in a reef mosaic. *Estuarine, Coastal and Shelf Science*, 101, 54-63

Barrier, N., Petrenko, A., & Ourmières, Y. 2016. Strong intrusions of the Northern Mediterranean Current on the eastern Gulf of Lion: insights from in-situ observations and high resolution numerical modelling. *Ocean Dynamics,* 66, 313-327 , doi: 10.1007/s10236-016-0921-7

Beckmann, A., & Haidvogel, D.B. 1993. Numerical simulation of flow around a tall isolated seamount. Part I : Problem formulation and model accuracy. *Journal Physical Oceanography,* 23, 1736-1752.

Bentsen, M., Evensen, G., Drange, H., & Jenkins, A.D. 1999 Coordinate transformation on a sphere using conformal mapping. *Monthly Weather Review*, 127(12), 2733-2740, doi:10.1175/1520-0493(1999)127.

Blayo, E., & Debreu, L. 1999: Adaptative mesh refinement for finite-difference ocean models: first experiments. *Journal Physical Oceanography*, 29, 1239-1250.

Bocaletti, S., Latora, V., & Moreno, Y. 2010 Handbook on Biological networks. World Scientific Lecture Notes in Complex Systems - vol. 10. World Scientific Publishing.

Cowen, R. K., Lwiza, K.M.M., Sponaugle, S., Paris, C.B., & Olson, D.B. 2000. Connectivity of marine populations: Open or closed? *Science*, 287(5454), 857-859

Cowen, R.K., Paris, C.B., & Srinivasan, A. 2006. Scaling of connectivity in marine populations. *Science*, 311 (5760), 522-527.

Denniss, T., Middleton, J.H., & Manasseh, R. 1995. Recirculation in the lee of complicated headlands: A case study of Bass Point. *Journal Geophysical Research*, 100 (C8), 16,087-16,101

Di Franco, A., Coppini, G., Pujolar, J.M., De Leo, G.A., Gatto, M., Lyubartsev, V., al. ..., Guidetti, P. (2012) Assessing Dispersal Patterns of Fish Propagules from an Effective Mediterranean Marine Protected Area. *PLoS ONE*, 7(12), e52108. doi:10.1371/journal.pone.0052108

Doglioli, A.M., Griffa, A., & Magaldi, M.G. 2004. Numerical study of a coastal current on a steep slope in presence of a cape: The case of the Promontorio di Portofino. *Journal Geophysical Research*, 109, C12033, doi:10.1029/2004JC002422

Estournel, C., Durrieu de Madron, X., Marsaleix, P., Auclair, F., Julliand, C., & Vehil, R. 2003. Observation and modelisation of the winter coastal oceanic circulation in the Gulf of Lion under wind conditions influenced by the continental orography (FETCH experiment). *Journal Geophysical Research*, 108(C3), doi:10.1029/2001JC000825

Fichaux, N., Poglio, T., & Ranchin, T. 2005. Mapping offshore wind resources: synergetic potential of SAR and scatterometer data. *IEEE Journal Ocean Engineering*, 30(3), 516-525

Font, T., & Lloret, J. 2014. Biological and Ecological Impacts Derived from Recreational Fishing in Mediterranean Coastal Areas. *Reviews in Fisheries Science & Aquaculture*, 22(1), 73-85.

Graham, W.M., & Largier, J.L. 1997 Upwelling shadows as nearshore retention sites: the example of northern Monterey Bay. *Continental Shelf Research*, 17 (5), 509-532

Gori, A., Linares, C., Rossi, S., Coma, R., & Gili, J.M. 2007. Spatial variability in reproductive cycle of the gorgonians Paramuricea clavata and Eunicella singularis (Anthozoa, Octocorallia) in the Western Mediterranean Sea. *Marine Biology*, 151, 1571-1584

Guénard, V., Dobrinski, P., Caccia, J.L., Campistron, B., & Benech, B. 2005. An observational study of the mesoscale Mistral dynamics. *Boundary Layer Meteorology*, 115, 263-288

Guizien, K., Brochier, T., Duchêne, J.C., Koh, B.S., & Marsaleix, P. 2006. Dispersal of Owenia fusiformis larvae by wind-driven currents: turbulence, swimming behaviour and mortality in a three-dimensional stochastic model. *Marine Ecology Progress Series*, 311, 47-66

Guizien, K., Belharet, M., Marsaleix, P., & Guarini, J.M. 2012. Using larval dispersal simulations for marine protected area design: Application to the Gulf of Lions (northwest Mediterranean). *Limnology Oceanography*, 57(4), 1099-1112 doi:10.4319/lo.2012.57.4.1099

Guizien, K., Belharet, M., Guarini, J.M., & Moritz, C. 2014. Marine benthic metapopulations vulnerability: implications of spatially structured connectivity for conservation practice. *Diversity and Distributions*, 20, 1392-1402 doi:10.1111/ddi.12254

Halpern, B.S., & Warner, R.R. 2003. Matching marine reserve design to reserve objectives *Proceedings Royal Society London B*, 270,1871-1878, doi 10.1098/rspb.2003.2405

Hamon, M., Beuvier, J., Somot, S., Lellouche, J.-M., Greiner, E., Jord, G., Drevillon,…, Drillet, Y. 2016. Design and validation of MEDRYS, a Mediterranean Sea reanalysis over 1992-2013. *Ocean Science*, 12, 577-599, doi:10.5194/os-12-577-2016

Hastings, A., & Botsford, L.W. (2006) Persistence of spatial populations depends on returning home. *Proceedings of National Academy of Science of USA*,103(15), 6067-6072.

Herbert, R.J.H., Willis, J., Jones, E., Ross, K., Hübner, R., Humphreys, J., A…, Baugh, J. 2012. Invasion in tidal zones on complex coastlines: modelling larvae of the non-native Manila clam, Rudipates philippinarum, in the UK. *Journal Biogeography*, 39, 585-599

Hong, J.S. 1980. Etude faunistique dun fond de concrétionnement de type coralligène soumis un gradient de pollution en Méditerranée nord-occidentale (Golfe de Fos). Thèse de Doctorat. Université d'Aix Marseille II.

Hu, Z. Y., Petrenko, A. A., Doglioli, A. M., & Dekeyser, I. 2011. Numerical study of eddy generation in the western part of the Gulf of Lion, *Journal Geophysical Research*, 116, C12030, doi:10.1029/2011JC007074.

Hua, B.L., & Thomasset, F. 1983. A numerical study of the effects of coastline geometry on wind-induced upwellings in the Gulf of Lions. *Journal Physical Oceanography*, 13, 678-694.

626 IUCN World Commission on Protected Areas (IUCN-WCPA) 2008. Establishing Marine Protected
627 Area Networks Making It Happen. Washington, D.C.: IUCN-WCPA, National Oceanic and
628 Atmospheric Administration and The Nature Conservancy. 118 p.
629
630 Johns, B., Marsaleix, P., Estournel, C., & Véhil, R., 1992. On the wind-driven coastal upwelling in
631 the Gulf of Lions. *Journal Marine System*, 3, 309-320
632
633 Lambrechts, J., Harnet, E., Deleersnijder, E., Bernard, P.E., Legat, V., Remacle, J.F., Wolanski, E.,
634 2008. A multi-scale model of the hydrodynamics of the whole Great Barrier Reef. *Estuarine,*
635 *Coastal and Shelf Science*, 79, 143-151.
636
637 Laubier, L. 1966. Le coralligène des Albères: monographie biocénotique. *Annales de l'Institut*
638 *Océanographique de Monaco*, 43, 139316
639
640 Levins, R. 1969. Some demographic and genetic consequences of environmental heterogeneity for
641 biological control. *Bulletin of the Entomology Society of America*, 71, 237-240
642
643 Mace, A.J., & Morgan, S.G. 2006. Larval accumulation in the lee of a small headland: implications
644 for the design of marine reserves. *Marine Ecology Progress Series*, 318, 19-29.
645
646 MAPAMED. 2016. Base de données des sites d'intérêt pour la conservation de l'environnement
647 marin en Méditerranée. MedPAN, PNUE/PAM/CAR-ASP.
648
649 Mariani, S., Uris, M. J., & Turon, X. 2005. The dynamics of sponge larvae assemblages from north-
650 western Mediterranean nearshore bottoms. Journal Plankton Research, 27(3), 249-262.
651
652 Marsaleix, P., Auclair, F., Floor, J.W., Herrmann, M.J., Estournel, C., Pairaud, I., & Ulses, C. 2008.
653 Energy conservation issues in sigma-coordinate free-surface ocean models. *Ocean Modelling*, 20,
654 61-89. http://dx.doi.org/10.1016/j.ocemod.2007.07.005.
655
656 Michaud H., Marsaleix, P., Leredde, Y., Estournel, C., Bourrin, F., Lyard, F., Mayet, C., &
657 Ardhuin, F., 2012. Three-dimensional modelling of wave-induced current from the surf zone to the
658 inner shelf. *Ocean Science*, 8, 657-681, doi:10.5194/os-8-657-2012.
659

Millazo, M., Chemello, R., Badalamenti, F., Camarda, R., Riggio, S. 2002. The impact of human recreational activities in Marine Protected Areas: what lessons should be learnt in the Mediterranean sea ? *Marine Ecology*, 23(1), 280-290.

Millot, C. 1979. Wind induced upwellings in the Gulf of Lions. *Oceanologica Acta*, 2(3), 261-274.

Millot, C., & Wald, L. Upwelling in the Gulf of Lions. F.A. Richards. Coastal Upwelling, 1981, United States. American Geophysical Union, 1, pp.160-166, 1981, Coastal and Estuarine Science Series.

Millot, C. 1990. The Gulf of Lion's hydrodynamics. *Continental Shelf Research,* 10(9-11), 885-894.

Moilanen, A. (2011) On the limitations of graph-theoretic connectivity in spatial ecology and conservation. *Journal Applied Ecology*, 48, 1543-1547.

Myksvoll, M. S., Jung, K-M., Albretsen, J., & Sundby, S. 2014. Modelling dispersal of eggs and quantifying connectivity among Norwegian coastal cod subpopulations. *ICES Journal of Marine Science*, 71, 957-969.

Nicolle, A., Dumas, F., Foveau, A., Foucher, E., & Thiébaut, E. 2013. Modelling larval dispersal of the king scallop (Pecten maximus) in the English Channel: examples from the bay of Saint-Brieuc and the bay of Seine. *Ocean Dynamics*, 63, 661-678 DOI 10.1007/s10236-013-0617-1.

Padron, M., & Guizien, K. 2016. Modelling the effect of demographic traits and connectivity on the genetic structuration of marine metapopulations of sedentary benthic invertebrates. *ICES Journal of Marine Science*, 73(7), 1935-1945. doi: 10.1093/icesjms/fsv158.

Petrenko, A.A. 2003. Variability of circulation features in the Gulf of Lion NW Mediterranean Sea. Importance of inertial currents. *Oceanologica Acta,* 26, 323-338.

Petrenko, A.A., Dufau, C., & Estournel, C. 2008. Barotropic eastward currents in the western Gulf of Lion, north-western Mediterranean Sea, during stratified conditions. *Journal of Marine Systems*, 74, 406-428, doi:10.1016/j.jmarsys.2008.03.004.

695 Putman, N.F., & He, R. 2013. Tracking the long-distance dispersal of marine organ- sensitivity to
696 ocean model resolution. *Journal Royal Society Interface*, 10, 20120979,
697 http://dx.doi.org/10.1098/rsif.2012.0979.
698
699 Roberts, C. M. 1997. Connectivity and management of Carribean coral reefs. *Science*, New Series,
700 278 (5342), 1454-1457.
701
702 Rossi, V., Ser Giacomi, E., Lopez Cristobal, A.A., & Hernandez-Garcia, E. 2014. Hydrodynamic
703 provinces and oceanic connectivity from a transport network help designing marine reserves.
704 *Geophysical Research Letter,* 9(41), 2883-2891.
705
706 Roughan, M., Mace, A. J., Largier, J. L., Morgan S. G. , Fisher, J. L., & Carter, M. L. 2005.
707 Subsurface recirculation and larval retention in the lee of a small headland: A variation on the
708 upwelling shadow theme. *Journal Geophysical Research, 110*, C10027,
709 doi:10.1029/2005JC002898.
710
711 Sala, E., Garrabou, J., & Zabala, M. 1996. Effects of diver frequentation on Mediterranean
712 sublittoral populations of the bryozoan Pentapora fascialis. *Marine Biology*, 126, 451-459.
713
714 Santangelo, G., Carletti, E., Maggi, E., & Bramanti, L. 2003. Reproduction and population sexual
715 structure of the overexploited Mediterranean red coral Corallium rubrum. *Marine Ecology Progress*
716 *Series*, 248, 99-108.
717
718 Soufflet, Y., Marchesiello, P., Lemarié, F., Jouanno, J., Capet, X., Debreu, L., & Benshila, R. 2016.
719 On effective resolution in ocean models. *Ocean Modelling*, 98, 36-50.
720
721 True, M. A. 1970. Etude quantitative de quatre peuplement sciaphiles sur substrat rocheux dans la
722 région marseillaise. *Bulletin Institut Oceanographique Monaco*, 69(1401), 1-48.
723
724 Xu, J., Yin, K., Liu, H., Lee, J. H. W., Anderson, D. M., Ho, A. Y. T., & Harrison, P. 2010. A
725 comparison of eutrophication impacts in two harbours in Hong Kong with different hydrodynamics.
726 *Journal of Marine System*, 83 (3-4),276-286.
727
728
729

List of Figures

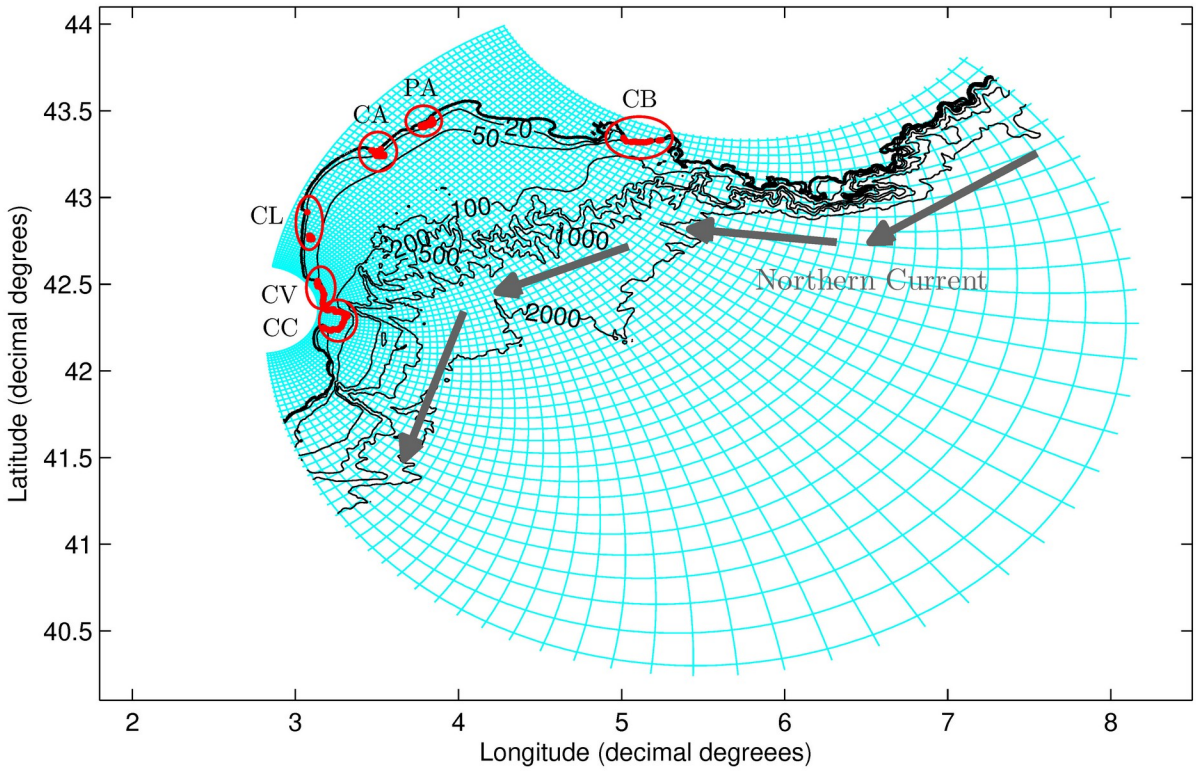

Figure 1 : Spatial extent of the simulated domain with the dipolar grid (680 × 710; 1 blue line every 10 cells) and the 20 m, 50 m, 100 m, 200 m, 500 m, 1000 m and 2000 m bathymetric contours. Parameters for the projection were: North pole (44.2° N ; 5.3° E) at indices (170; 710); South pole (42.37° N; 2.82° E); reference latitude for Mercator projection was 52° N. The 6 rocky habitats (CC= Cap de Creus, CV= Côte Vermeille, CL= Cap Leucate, CA= Cap d'Agde, PA= Plateau des Aresquiers, CB= Côte Bleue) are indicated in red and the coastline is depicted by a bold line.

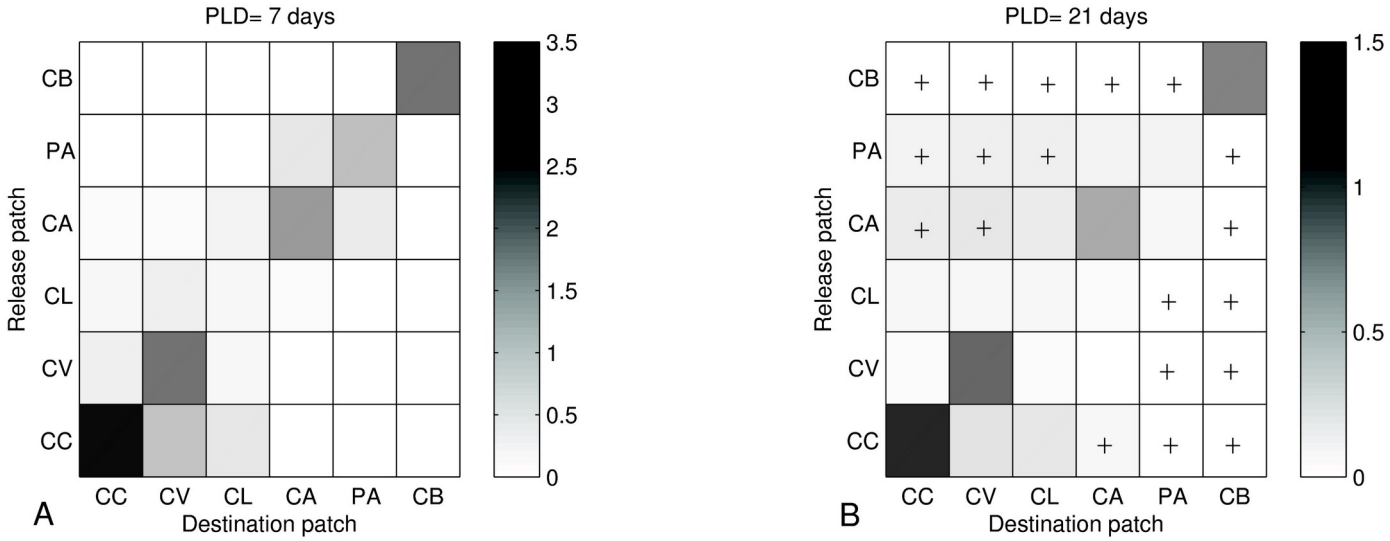

Figure 2 : Connectivity matrices containing mean transfer rates (in %) computed for the summer seasons of 2010, 2011 and 2012 between the 6 main rocky habitat patches of the Gulf of Lion (CC= Cap de Creus, CV= Côte Vermeille, CL= Cap Leucate, CA= Cap d'Agde, PA= Plateau des Aresquiers, CB= Côte Bleue) (A) for a 7-day PLD and (B) for a 21-day PLD. Symbol (+) display those transfer rates that increased in the 21-day PLD compared to the 7-day PLD.

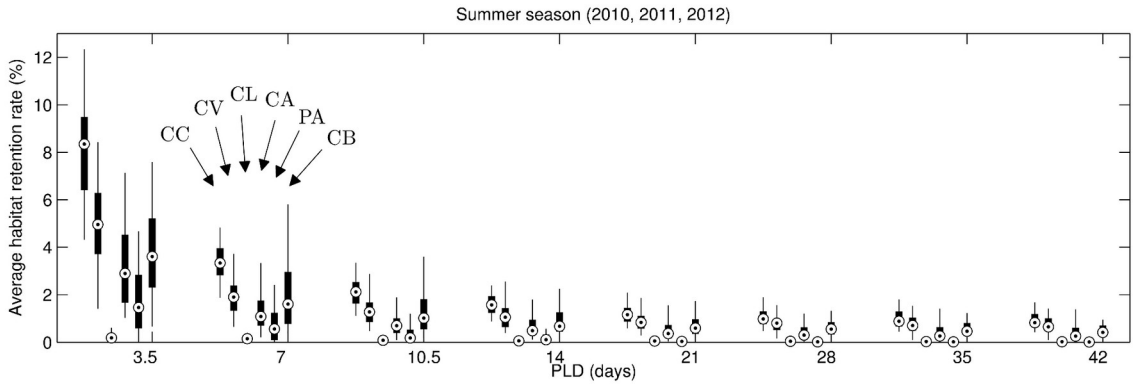

Figure 3 : Boxplots of the mean retention rate in the six main rocky habitat patches (CC= Cap de Creus, CV= Côte Vermeille, CL= Cap Leucate, CA= Cap d'Agde, PA= Plateau des Aresquiers, CB= Côte Bleue) computed for the thirteen 1-week release periods in 3 consecutive years (2010, 2011 and 2012) and for dispersal duration ranging from 3.5 days to 42 days.

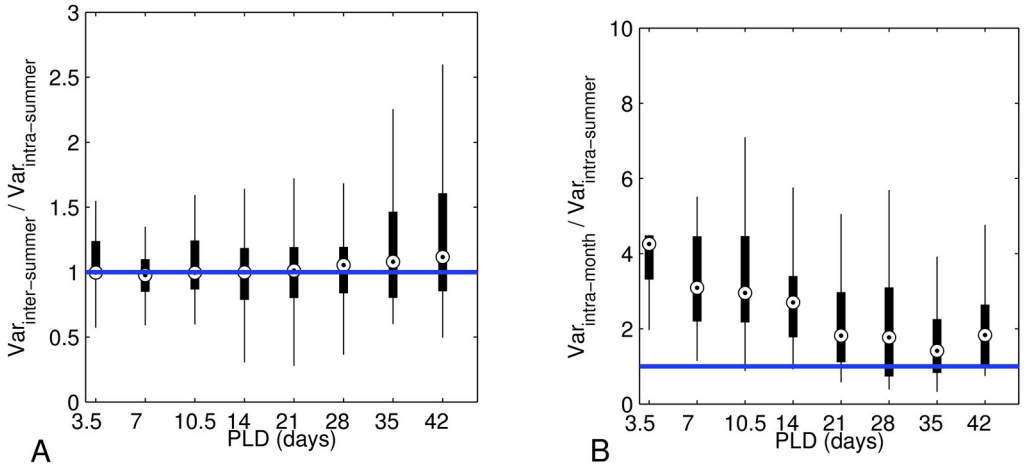

Figure 4 : Boxplot of (A) $Var_{inter\text{-}summer}$ /$Var_{intra\text{-}summer}$ ratio and (B) $Var_{intra\text{-}month}$ /$Var_{intra\text{-}summer}$ ratio of any element in the connectivity matrices computed for the thirteen 1-week release periods in 3 consecutive years (2010, 2011 and 2012) and for PLD ranging from 3.5 days to 42 days.

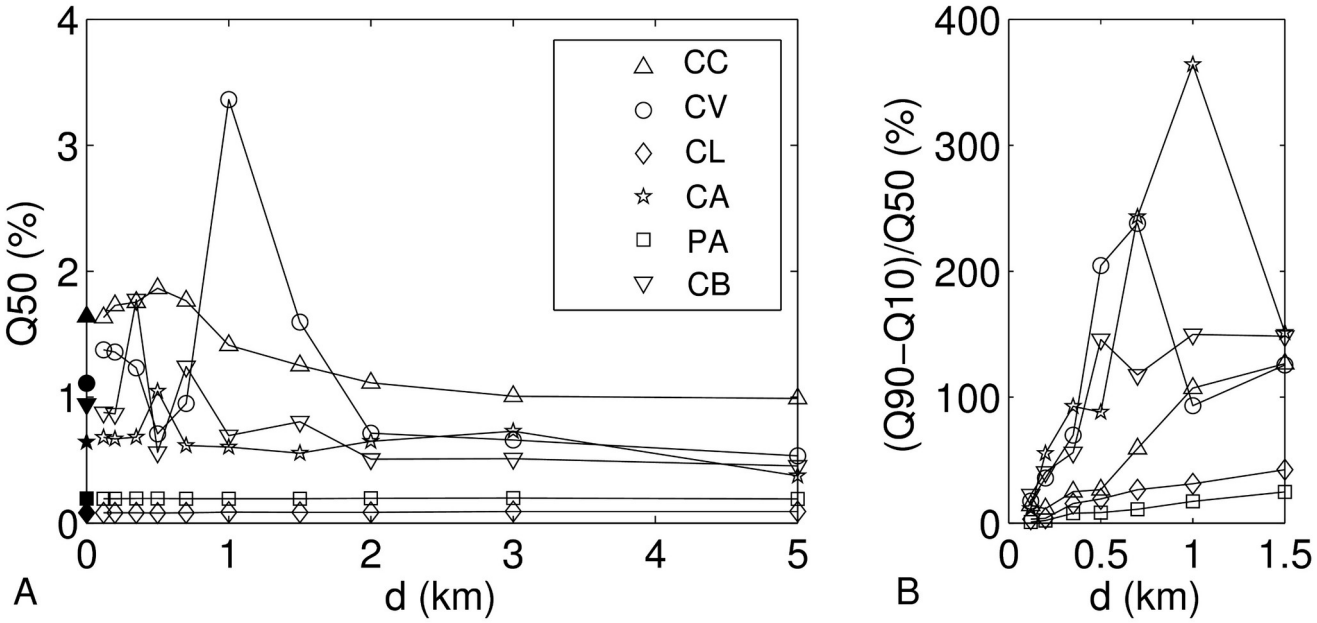

Figure 5 : (A) Median Q_{50} retention rate at habitat patch scale versus minimal distance between release spots *d* for each habitat and a 21-day PLD (open symbols, CC= Cap de Creus, CV= Côte Vermeille, CL= Cap Leucate, CA= Cap d'Agde, PA= Plateau des Aresquiers, CB= Côte Bleue). Filled symbols indicates the retention rate when all release spots are considered. (B) Difference $Q_{90} - Q_{10}$ as percentage of the median Q_{50} for each distance *d*.

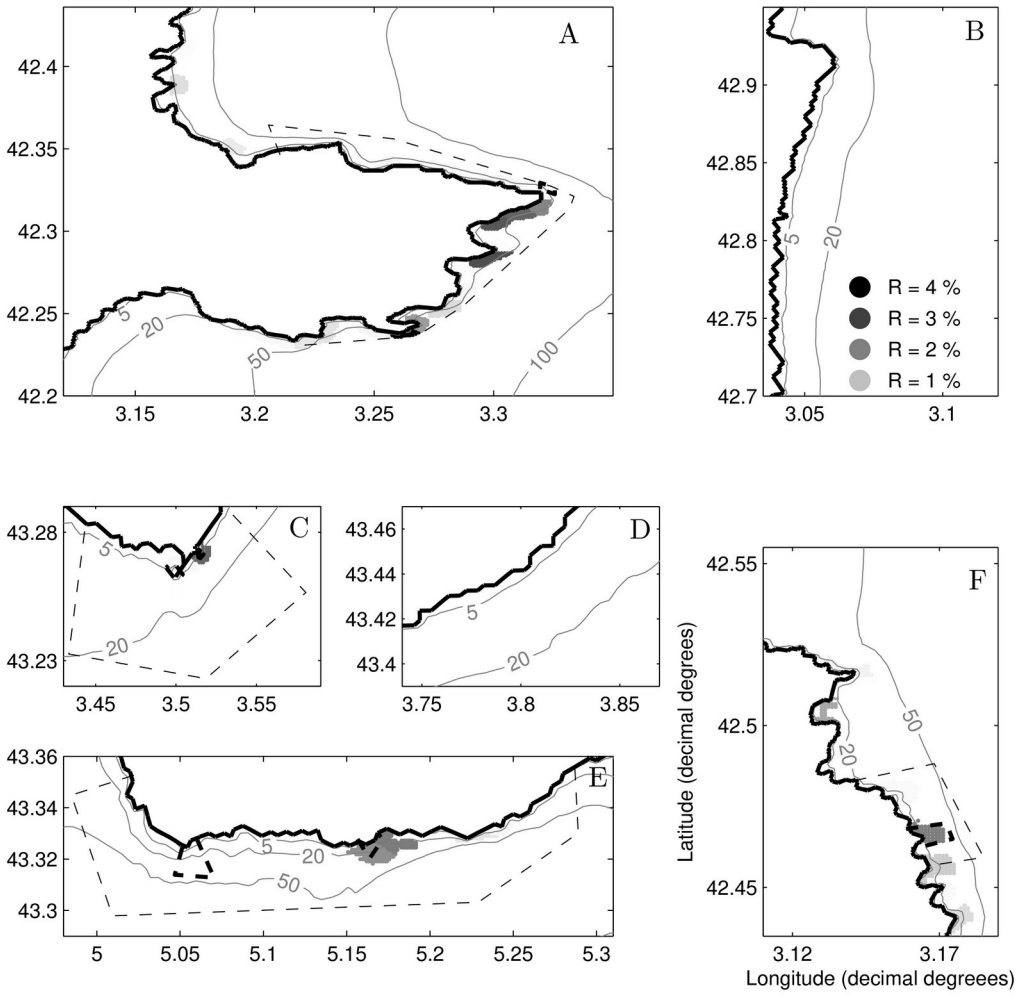

Figure 6 : Each panel is a close up of one of the six main rocky habitat patch showing the average retention rate over three years (2010, 2011 and 2012) in each of the 115 subpatches for a 21-day PLD (bold dots). A displays Cap de Creus, B displays Cap Leucate, C displays Cap d'Agde, D displays Plateau des Aresquiers, E displays Côte Bleue and F displays Côte Vermeille. Bathymetric contours are displayed in gray and labeled in meters, and coastline is displayed by the black thick line. Thin dashed line delimitates the areas designated for marine protection. Thick dashed line delimitates the areas where special protection is implemented.

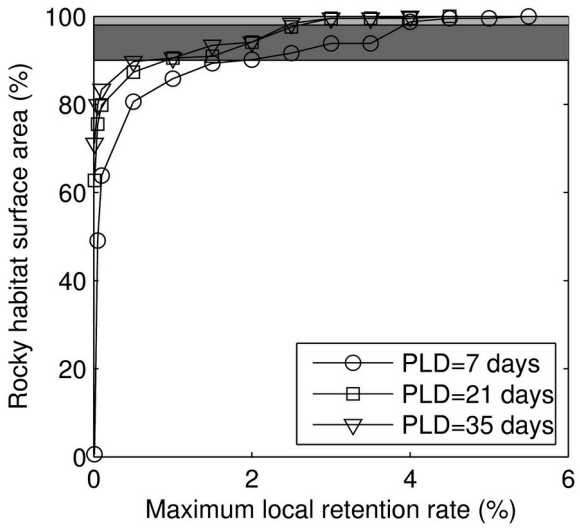

Figure 7 : Cumulative area distribution of local retention rate in the rocky habitat of the Gulf of Lion for a PLD of 1 week (circle), 3 weeks (square), and 5 weeks (triangle). Shaded dark grey area displays the maximum local retention values if the 10% MPA coverage extent targetted by the 10th United Nations Conference of the Parties for 2020 concerned the most retentive subpatches in the Gulf of Lion. Shaded light grey area displays the maximum local retention values if the 2% no-take zones coverage extent targetted by the MEDPAN Forum for 2020 concerned the most retentive subpatches in the Gulf of Lion.

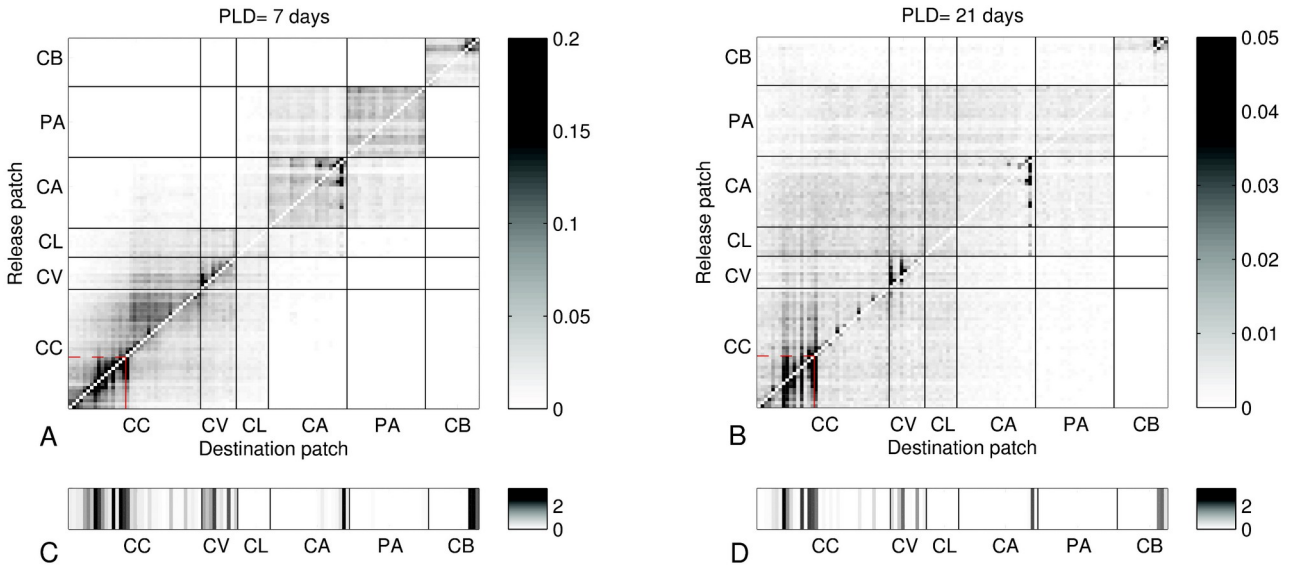

Figure 8 : Average connectivity matrices between 115 subpatches of 1-km^2 for summer 2010, 2011 and 2012 for a 7-day PLD (A and C) and for a 21-day PLD (B and D). To give more visibility to transfer rates between subpatches, (A) and (B) displays transfer rates between subpatches only (outside diagonal), and (C) and (D) displays the local retention in each subpatch (values on the diagonal). Horizontal and vertical lines delimitate the six main rocky habitat patches (CC= Cap de Creus, CV= Côte Vermeille, CL= Cap Leucate, CA= Cap d'Agde, PA= Plateau des Aresquiers, CB= Côte Bleue) used to establish low-resolution connectivity matrices. The southern part of the Cap de Creus is delineated with red dashed lines. Transfer rates are in %.

List of Tables

	Cap de Creus	Côte Vermeille	Cap Leucate	Cap d'Agde	Plateau des Aresquiers	Côte Bleue
Number of release spots	2085	421	654	1638	1595	1041
d=120m	1026 (175)	215 (57)	322 (29)	794 (449)	777 (83)	516 (36)
d=200m	524 (869)	115 (193)	162 (369)	394 (1107)	402 (869)	266 (471)
d=350m	189 (1591)	48 (295)	51 (585)	121 (1546)	119 (1505)	93 (832)
d=500m	102 (1818)	31 (358)	28 (551)	68 (1426)	67 (1245)	55 (817)
d=700m	64 (1897)	21 (340)	16 (571)	36 (1593)	35 (1434)	33 (860)
d=1km	42 (1891)	12 (320)	9 (570)	20 (1467)	18 (1457)	20 (882)
d=1.5km	27 (1892)	8 (326)	5 (494)	10 (1443)	10 (1509)	13 (822)
d=2km	20 (1947)	5 (323)	4 (583)	7 (1602)	6 (1456)	10 (841)
d=3km	13 (1877)	4 (314)	2 (583)	4 (1518)	3 (1333)	6 (859)
d=5km	7 (1920)	2 (305)	2 (653)	2 (1509)	2 (1220)	4 (819)
RO_{7days}(%)	22	34	74	31	32	0
RO_{21days}(%)	18	25	76	48	82	7

Table 1 : First line indicates the original number of release spots regularly distributed over a 100 m by 100 m grid for each habitat. Following lines provide the mean number of release spots per subset, and between parenthesis the number of different subsets that were found for each minimum distance d. Last two lines gives the relative out-strength values calculated for a 1 week and a 3 week dispersal duration for each habitat.

Supplementary Material 1 to High resolution modelling of ocean circulation can reveal retention spots important for biodiversity conservation: Sensitivity of retention rate to release spots spatial distribution

Florence Briton [1], Daphne Cortese [1], Thomas Duhaut [2], Katell Guizien [1],*

[1] CNRS, Sorbonne Universités (UPMC Univ Paris 06), Laboratoire d'Ecogochimie des Environnements Benthiques (LECOB), Observatoire Ocanologique, Banyuls/Mer, F-66650, France

[2] CNRS, Université de Toulouse, Laboratoire d'Aérologie de Toulouse, 14 avenue E. Belin - Toulouse, F-31400, FRANCE

* guizien@obs-banyuls.fr

Thanks to the high resolution of flow simulations (less than 300 m in each habitat patch), the sensitivity of habitat patch retention rate estimates to the spatial density of release spots (hereafter indicated by release spot distance) could be reliably assessed. The robustness of habitat patch retention rate estimates was determined by two criteria: the reduction of the uncertainty defined as the relative interquantile range $(Q_{90} - Q_{10})/Q_{50}$ and the stabilization of the median value Q_{50} of retention rate frequency distribution. As an example, in the Cap de Creus habitat patch, with low density of release spot (d=1500m , d=700m, Fig.1B and D), local retention rates are quite evenly distributed across a wide range of values, and the mode does not appear (Fig.1A and C): the median retention rate is not representative and increased from 1.85% for d=1500m to 2.47% for d=700m. For a minimum distance of 500m between release spots (Fig.1F, H and J), the mode emerges, and the quantiles Q_{10} and Q_{90} get closer to the median (Fig.1E, G and I). Both stabilization of the median value Q_{50} and reduction of the relative interquantile range $(Q_{90} - Q_{10})/Q_{50}$ (herein called uncertainty) when release spot distance decreases define the convergence toward a stable unimodal

distribution. Convergence is reached when uncertainty becomes lower than 20% and the retention rate of the habitat is estimated by the median value of the converged distribution (Fig.1G).

The contribution of each release spot to the retention rate of the habitat patch it belongs to was calculated as the proportion of particles released in that spot during a release event that came back into its original habitat patch after a certain PLD. The history of the particle contributing to the local retention was investigated as well. Indeed, local retention can result from two different processes. Either the particles remained in the patch where they were released, kept by local hydrodynamics structures, or they are swept away from their release patch and find their way back through meso-scale recirculation structures. To arbitrate between the two possibilities, for each release spot the proportion of particles released there that contributed to the local retention staying in the patch during the whole dispersal period was also calculated.

As an example, Supplementary Figure 2 displays the spatial distribution of the release spots having the highest retention rates in the habitat and cumulating 75% of the habitat patch retention rate for a 21-day PLD. These release spots were evenly distributed and represented 41% and 51% of the release spots in Plateau des Aresquiers and Cap Leucate, respectively. In Cap de Creus, 75% of the habitat patch retention rate is accounted for by 31% of the release spots which were regularly distributed along the southern half of the habitat. In contrast, 75% of the habitat patch retention rate was accounted for by only 17% of the release spots in Côte Vermeille, 16% in Cap d'Agde, and 3% in Côte Bleue. The latters were sometimes isolated but more often accumulated in subpatches of ten or more release spots. In Côte Vermeille, those spots were located around bays and capes. In Côte Bleue, there were a few retention pools close to the shore but in steep bathymetry in its eastern part. In Agde, they were concentrated near the coast at depths less than 5m. The most retentive release spots did not vary for PLDs larger than 21 days in Cap de Creus, Côte Vermeille, Cap d'Agde and Côte Bleue (Supplementary Figures 3 and 4) indicating that particles released in those most retentive spots did not leave the habitat patch during their dispersal period. In contrast, in Cap Leucate and Plateau des Aresquiers, no particles remained in their original habitat patch during their whole dispersal period (data not shown), and the ones contributing to habitat patch retention depended only on recirculation structures to return to their original habitat. This analysis guided the definition of 115 subpatches ranging in area from 0.16 to 1.4 km^2 (0.66 km^2 on average), in which retention rate was spatially homogeneous (Supplementary Figures 5).

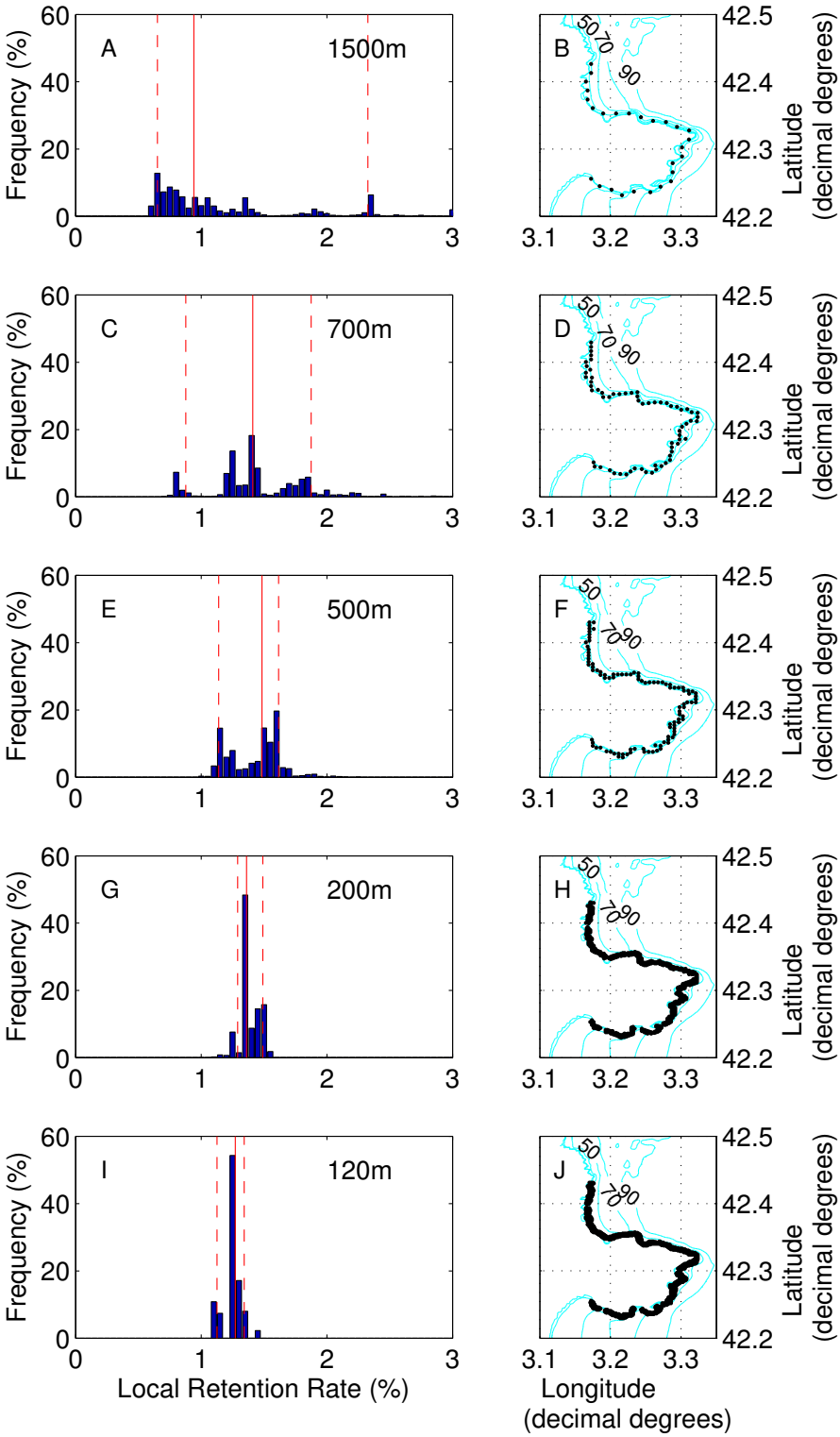

Supplementary Figure 1: Frequency distributions of local retention rates at Cap de Creus for increasing density of release sites (A: d=1.5km; C: d=700m; E: d=500m; G: d=200m; I: d=120m, where d is the distance between release sites). For each release spatial density, the number of samples is equal to the number of subsets that could be made from the original distribution at 100m resolution as indicated in Table 1. The solid line represents the median value Q50, and the dashed lines the quantiles Q_{10} and Q_{90}. A sample of a release sites subset for each release spatial density is mapped on the right panels (B: d=1.5km; D: d=700m; F: d=500m; H: d=200m; J: d=120m).

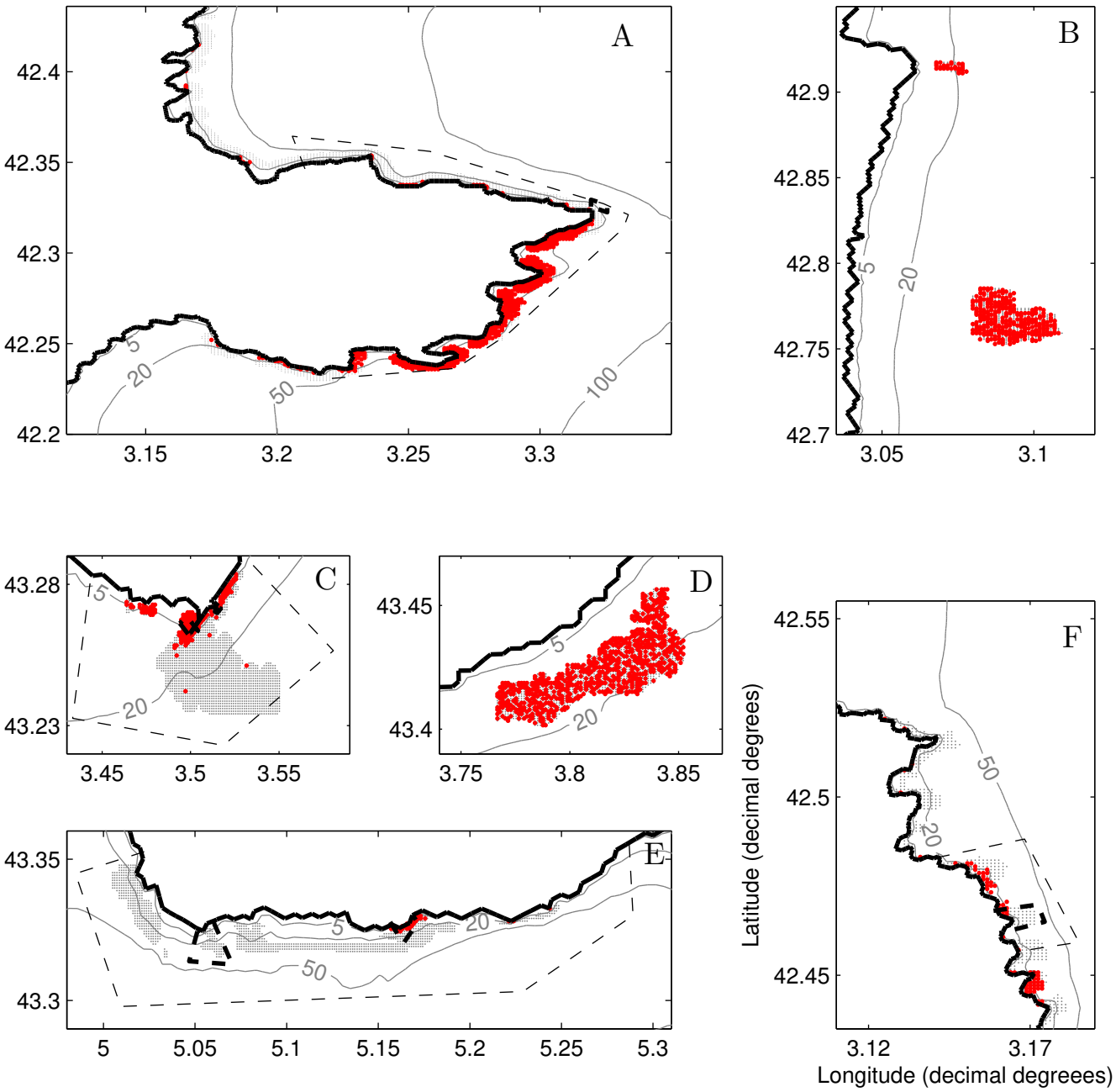

Supplementary Figure 2: Each panel is a close up of one of the six main rocky habitat patch showing the distribution of release spots spaced by a 100 m (small grey dots) and the most retentive release spots accounting for 75% of the average habitat retention rate over the summer of 2010, 2011 and 2012 for a 21-day PLD (bold red dots). A displays Cap de Creus, B displays Cap Leucate, C displays Cap d'Agde, D displays Plateau des Aresquiers, E displays Côte Bleue and F displays Côte Vermeille. Bathymetric contours are displayed in gray and labeled in meters, and coastline is displayed by the black thick line. Thin dashed line delimitates the areas designated for marine protection. Thick dashed line delimitates the areas where special protection is implemented.

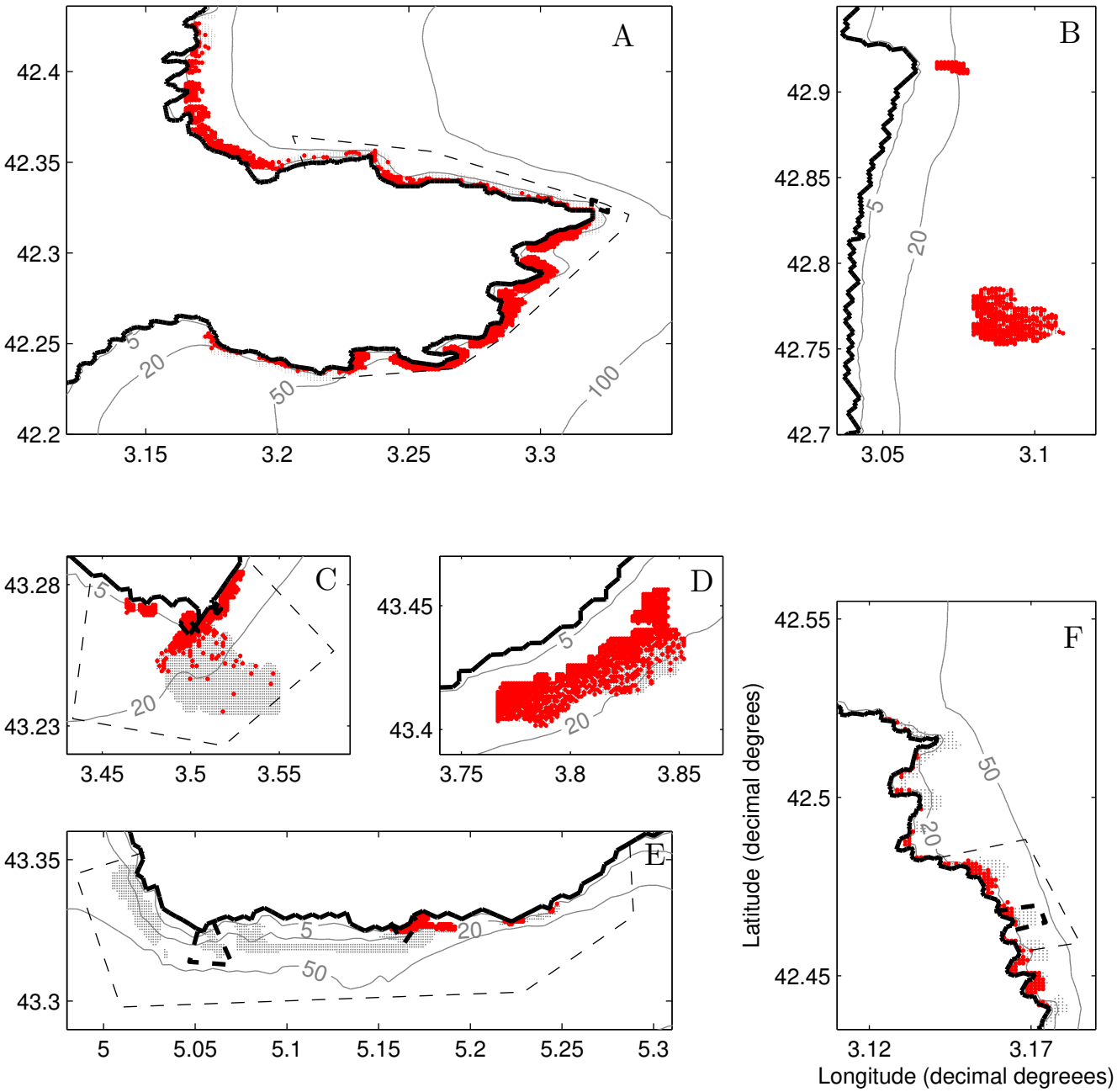

Supplementary Figure 3: Same as Figure 2 but for a 7-day PLD.

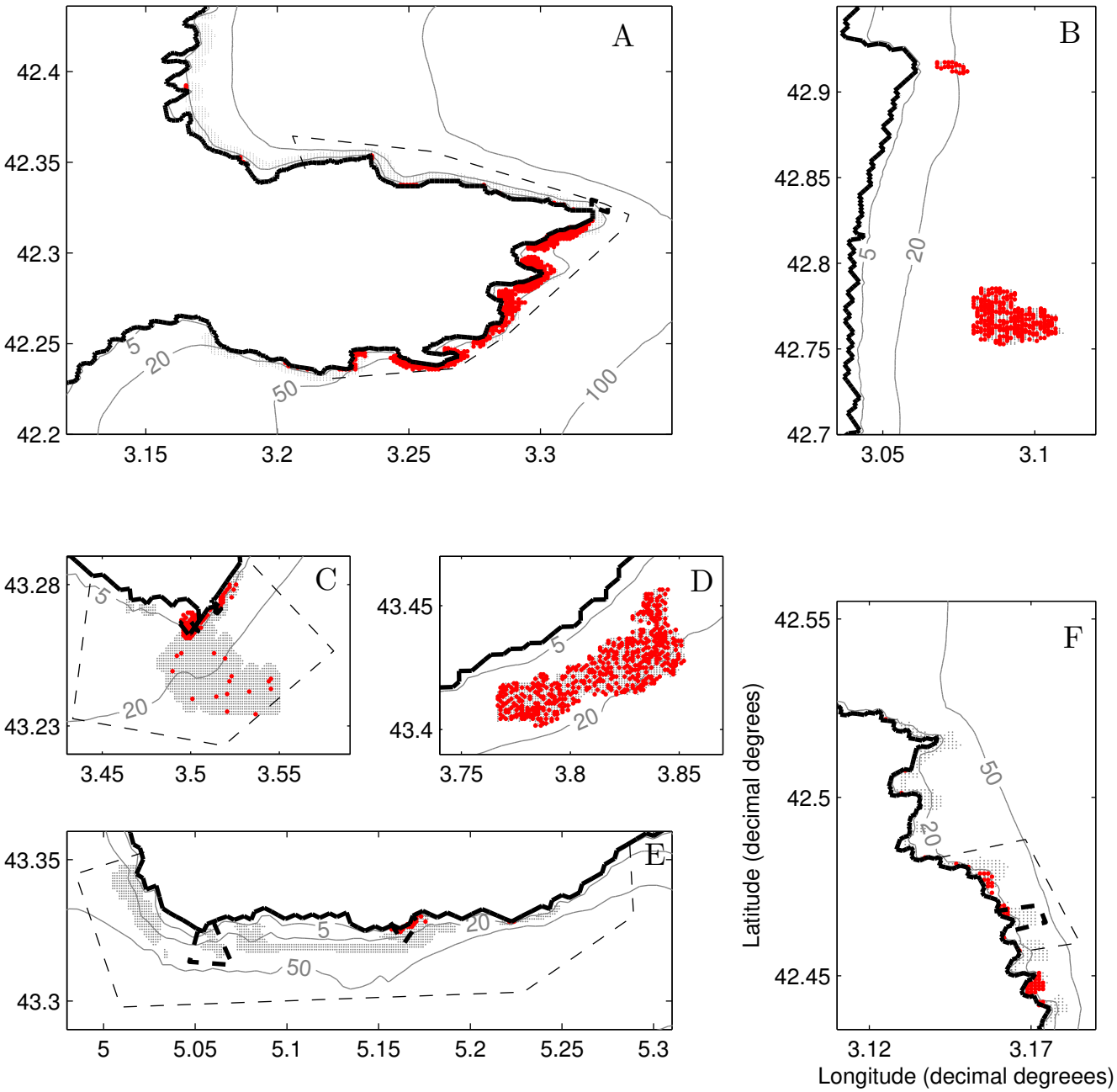

Supplementary Figure 4: Same as Figure 2 but for a 35-day PLD.

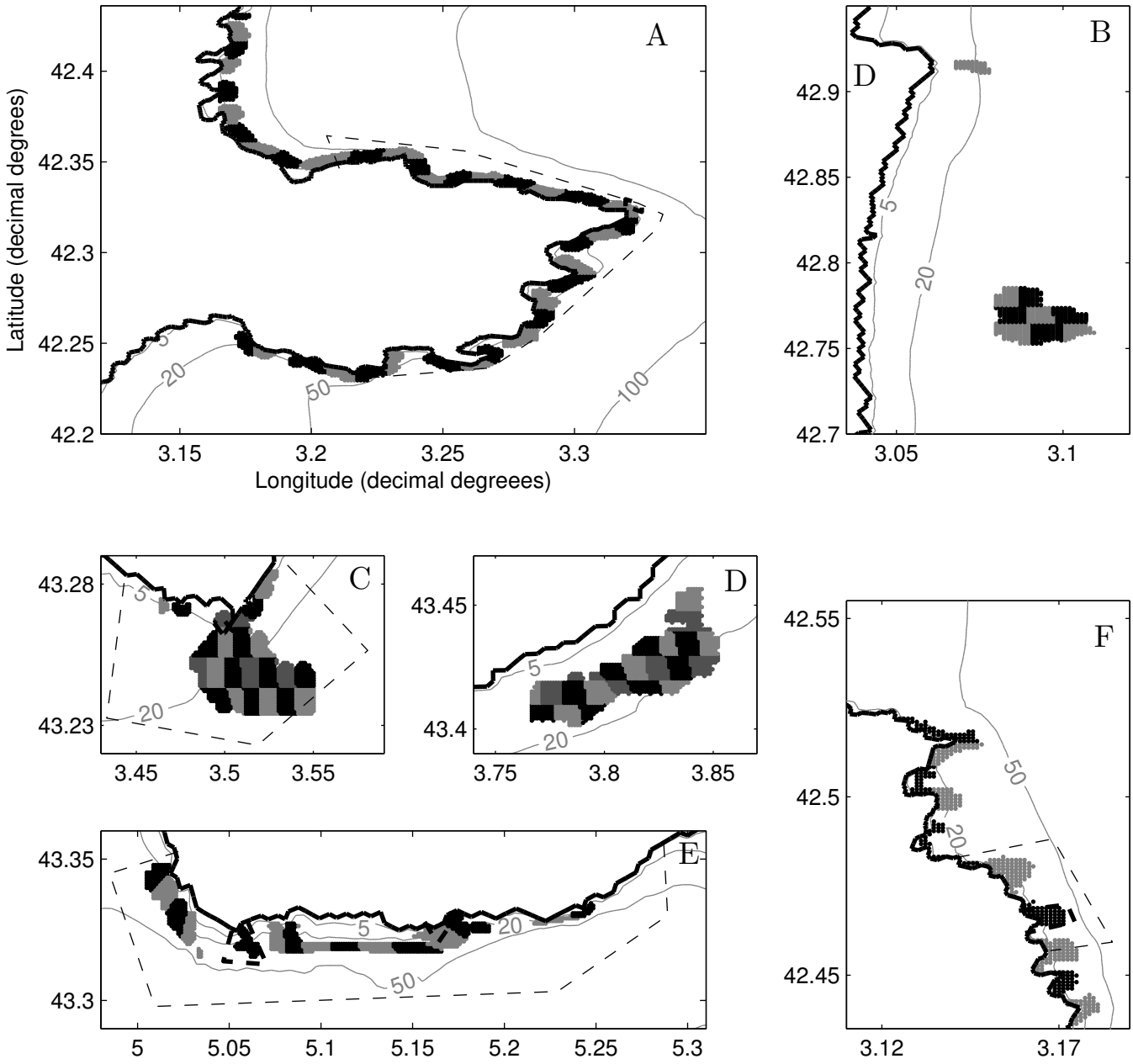

Supplementary Figure 5: Each panel is a close up of one of the six main rocky habitat patch showing the distribution of 115 subpatches of about 1-km^2 grouping release spots spaced by a 100 m. The subpatches are individuated by different gray intensity. Bathymetric contours are displayed in gray and labeled in meters, and coastline is displayed by the black thick line. Thin dashed line delimitates the areas designated for marine protection. Thick dashed line delimitates the areas where special protection is implemented.

Supplementary Material 2 to High resolution modelling of ocean circulation can reveal retention spots important for biodiversity conservation: Sensitivity of connectivity to release timing variability

Florence Briton [1], Daphne Cortese [1], Thomas Duhaut [2], Katell Guizien [1],*

[1] CNRS, Sorbonne Universités (UPMC Univ Paris 06), Laboratoire d'Ecogochimie des Environnements Benthiques (LECOB), Observatoire Ocanologique, Banyuls/Mer, F-66650, France

[2] CNRS, Université de Toulouse, Laboratoire d'Aérologie de Toulouse, 14 avenue E. Belin - Toulouse, F-31400, FRANCE

* guizien@obs-banyuls.fr

The 39 non-overlapping week-long release periods (13 per year in 3 years) defined in Supplementary Table 1 were used to calculate connectivity matrices for different week-long release periods. The meteorological, seasonal and climatic (inter-annual) variability was quantified by intra-month $\mathrm{Var}_{intra-month}$, intra-summer $\mathrm{Var}_{intra-summer}$ and inter-summer $\mathrm{Var}_{inter-summer}$ variabilities, respectiveley, and defined as follows:

Meteorological variability on any transfer rate T (anu element of the connectivity matrix) was quantified by the intra-month (i.e between release periods within each month of reproduction) variability of the transfer rate defined as:

$$\mathrm{Var}_{intra-month} = \frac{\sum_{y=1}^{N_{year}} \sum_{m=1}^{N_{month}} \left(\frac{\sum_{p=1}^{N_{period}} (T_{m,p}^{y} - \overline{T_m^y})^2}{N_{period}} \right)}{N_{year} N_{month}} \quad (1)$$

with the average transfer rate of month m in year y defined as:

$$\overline{T_m^y} = \frac{\sum_{p=1}^{N_{period}} T_{m,p}^y}{N_{period}} \tag{2}$$

Seasonality on any transfer rate T (any element of the connectivity matrix) was quantified by the intra-summer (i.e between different months of reproduction within a same year) variability of the transfer rate defined as:

$$\mathrm{Var}_{intra-summer} = \frac{\sum_{y=1}^{N_{year}} \left(\frac{\sum_{m=1}^{N_{month}} (\overline{T_m^y} - \overline{T^y})^2}{N_{month}} \right)}{N_{year}} \tag{3}$$

with the average connectivity matrix of year y defined as:

$$\overline{T^y} = \frac{\sum_{m=1}^{N_{month}} \overline{T_m^y}}{N_{month}} \tag{4}$$

Climatic variability on any transfer rate T (any element of the connectivity matrix) was quantified by the inter-summer (i.e between the same month of reproduction in different years) variability of the transfer rate defined as:

$$\mathrm{Var}_{inter-summer} = \frac{\sum_{m=1}^{N_{month}} \left(\frac{\sum_{y=1}^{N_{year}} (\overline{T_m^y} - \overline{T_m})^2}{N_{year}} \right)}{N_{month}} \tag{5}$$

with the average connectivity matrix of month m defined as:

$$\overline{T_m} = \frac{\sum_{y=1}^{N_{year}} \overline{T_m^y}}{N_{year}} \tag{6}$$

with $N_{year} = 3$ the number of years (2010, 2011, 2012), $N_{month} = 3$ the number of reproductive months (June, July, August), $N_{period} = 4$ the number of one-week long release periods per month. Thus, only the week-long release periods 1 to 12 (Table 1) were taken into account in the calculation of meteological, seasonal and inter-annual variability, in order to maintain a same number of periods per month.

	2010	2011	2012	Assigned reproductive month
Period 1	June, 6 to June,12	June, 5 to June, 11	June, 3 to June, 9	June
Period 2	June, 13 to June, 19	June, 12 to June, 18	June, 10 to June, 16	June
Period 3	June, 20 to June, 26	June, 19 to June, 25	June, 17 to June, 23	June
Period 4	June, 27 to July, 3	June, 26 to July, 2	June, 24 to June, 30	June
Period 5	July, 4 to July, 10	July, 3 to July, 9	July, 1 to July, 7	July
Period 6	July, 11 to July, 17	July, 10 to July, 16	July, 8 to July, 14	July
Period 7	July, 18 to July, 24	July, 17 to July, 23	July, 15 to July, 21	July
Period 8	July, 25 to July, 31	July, 24 to July, 30	July, 22 to July, 28	July
Period 9	August, 1 to August, 7	July, 31 to August, 6	July, 29 to August, 4	August
Period 10	August, 8 to August, 14	August, 7 to August, 13	August, 5 to August, 11	August
Period 11	August, 15 to August, 21	August, 14 to August, 20	August, 12 to August, 18	August
Period 12	August, 22 to August, 28	August, 21 to August, 27	August, 19 to August, 25	August
Period 13	August, 29 to September, 4	August, 28 to September, 3	August, 26 to September, 1	none

Supplementary Table 1: Starting and finishing date of the thirteen week-long release periods in the three consecutive years 2010, 2011 and 2012. Last column indicates the reproductive month to which each period was assigned for testing the intra-summer variability.